Emerging solvent-induced homochirality by the confinement of achiral molecules against a solid surface

Katsonis, Nathalie; Xu, Hong; Haak, Robert M.; Kudernac, Tibor; Tomovic, Zeljko; George, Subi; Van der Auweraer, Mark; Schenning, Albert P. H. J.; Meijer, E. W.; Feringa, Ben L.

Published in:
Angewandte Chemie-International Edition

DOI:
10.1002/anie.200800255

Angewandte Chemie
Eine Zeitschrift der Gesellschaft Deutscher Chemiker

Supporting Information

69451 Weinheim, Germany

Emerging solvent-induced homochirality by the confinement of achiral molecules against a solid surface**

Nathalie Katsonis, Hong Xu, Robert M. Haak, Tibor Kudernac, Željko Tomović, Subi George, Mark Van der Auweraer, Albert P. H. J. Schenning,* E. W. Meijer,* Ben L. Feringa,* and Steven De Feyter**

Organic Synthesis

Materials

Starting materials were purchased from Aldrich or Acros and used as received. Lipase from Pseudomonas cepacia was obtained from Fluka. All solvents were reagent grade and dried and distilled prior to use. Demineralized water was used in the preparation of all aqueous solutions. Column chromatography was performed on silica gel (Aldrich 60, 230-400 mesh). TLC was performed on silica gel 60/Kieselguhr F_{254}.

^{1}H and ^{13}C NMR spectra were recorded on a Varian VXR300 (299.97 MHz for ^{1}H, 75.48 MHz for ^{13}C) or a Varian AMX400 (399.93 MHz for ^{1}H, 100.59 MHz for ^{13}C) spectrometer in $CDCl_3$. Chemical shifts are reported in □ values (ppm) relative to the residual solvent peak ($CHCl_3$, ^{1}H = 7.24, ^{13}C = 77.0). Carbon assignments are based on APT ^{13}C experiments. Splitting patterns are indicated as follows: s (singlet), d (doublet), t (triplet), q (quartet), m (multiplet), br (broad).

Mass spectra (HRMS) were recorded on a Jeol JMS-600H.

HPLC analysis was performed on a Shimadzu HPLC system equipped with two LC-10AD *vp* solvent delivery systems, a DGU-14A degasser, a SIL-10AD *vp* auto injector, an SPD-M10A *vp* diode array detector, a CTO-10A *vp* column oven, and an SCL-10A *vp* system controller using the columns indicated for each compound separately.

Synthesis of the chiral solvents[1]

Racemic 1-phenyl-1-octanol was prepared by Grignard addition of heptyl magnesium bromide to benzaldehyde using standard techniques (Figure S1). Purification was achieved by column chromatography over SiO_2 (gradient heptane - heptane/EtOAc 9:1). To obtain samples for use in STM measurements, the compound was further purified by Kugelrohr distillation.

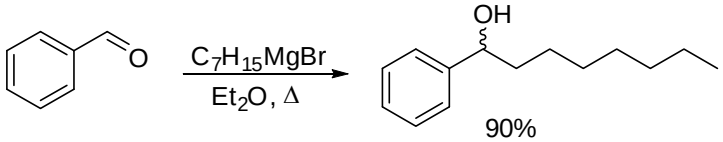

Figure S1 : Synthesis of *rac*-1-phenyl-1-octanol.

[1] K. Mori, R. Bernotas, *Tetrahedron: Asymm.* **1990**, *1*, 97-110.

^{1}H NMR ($CDCl_3$) δ 7.38-7.20 (m, 5H), 4.63 (dd, *J* = 7.3, 5.9 Hz), 1.90 (s, 1H), 1.83-1.62 (m, 2H), 1.44-1.16 (m, 10H), 0.86 (t, *J* = 6.6 Hz, 3H).

^{13}C NMR ($CDCl_3$) δ 144.9 (s), 128.4 (d), 127.4 (d), 125.9 (d), 74.7 (d), 39.1 (t), 31.8 (t), 29.5 (t), 29.2 (t), 25.8 (t), 22.6 (t), 14.0 (q).

MS (EI+): *m/z* = 206 (M^+), 188, 117, 107, 104, 82, 79, 77.

HRMS (EI+): calculated for $C_{14}H_{22}O$: 206.1671, found: 206.1681

Acetylation was achieved by subjecting 1-phenyl-1-octanol to acetic anhydride in pyridine at 0ºC overnight (Figure S2). The crude acetate thus obtained was purified using column chromatography over SiO_2 (eluent pentane - Et_2O 50:1).

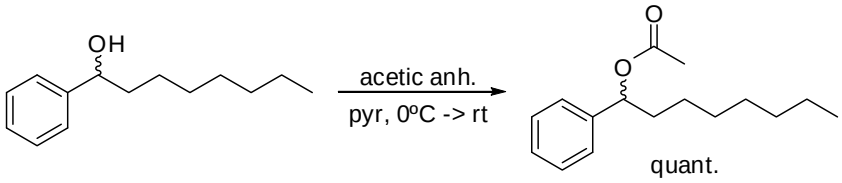

Figure S2 : Acetylation of 1-phenyl-1-octanol.

^{1}H NMR ($CDCl_3$) δ 7.35-7.25 (m, 5H), 5.72 (ddd, *J* = 7.7, 6.2, 1.5 Hz, 1H), 2.05 (d, *J* = 1.8 Hz, 3H), 1.97-1.85 (m, 1H), 1.80-1.70 (m, 1H), 1.38-1.15 (m, 10H), 0.86 (t, *J* = 6.6 Hz, 3H).

^{13}C NMR ($CDCl_3$) δ 170.3 (s), 140.9 (s), 128.3 (d), 127.8 (d), 126.5 (d), 76.14 (d), 36.3 (t), 31.7 (t), 29.3 (t), 29.1 (t), 25.5 (t), 22.6 (t), 21.2 (q), 14.0 (q).

MS (EI+): *m/z* = 248 (M^+), 206, 188, 149, 117, 107, 105, 104, 91.

HRMS (EI+): calculated for $C_{16}H_{24}O_2$: 248.1776, found: 206.1782

Enantiomerically pure 1-phenyl-1-octanol was prepared by applying the procedure of Mori and Bernotas[1] on a large scale (Figure S3). Thus, 20.5 mmol of 1-phenyloctyl acetate was dissolved in 100 mL of acetone and added to 900 mL of phosphate buffer (100 mM, pH 6.9). Furthermore, 40 drops of Triton-X100 were added. Finally, 1.94 g of ps. C. lipase was added. After 16 d, the mixture was extracted with Et_2O (3x), the combined organic layers were washed with a saturated solution of $NaHCO_3$ sat and brine, respectively, then filtered and the solvent was evaporated. Purification was achieved by column chromatography over SiO_2 using a gradient of pentane/Et_2O 19:1 – 1:1. The (*R*)-alcohol and (*S*)-acetate were further purified using kugelrohr distillation.

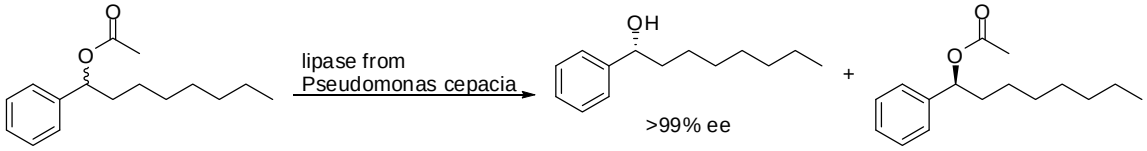

Figure S3 : Enzymatic kinetic resolution of 1-phenyl-1-octyl acetate.

Copies of relevant analytical data (^{1}H NMR and HPLC traces) for the solvents used in this study can be found in Figures S4 - S10.

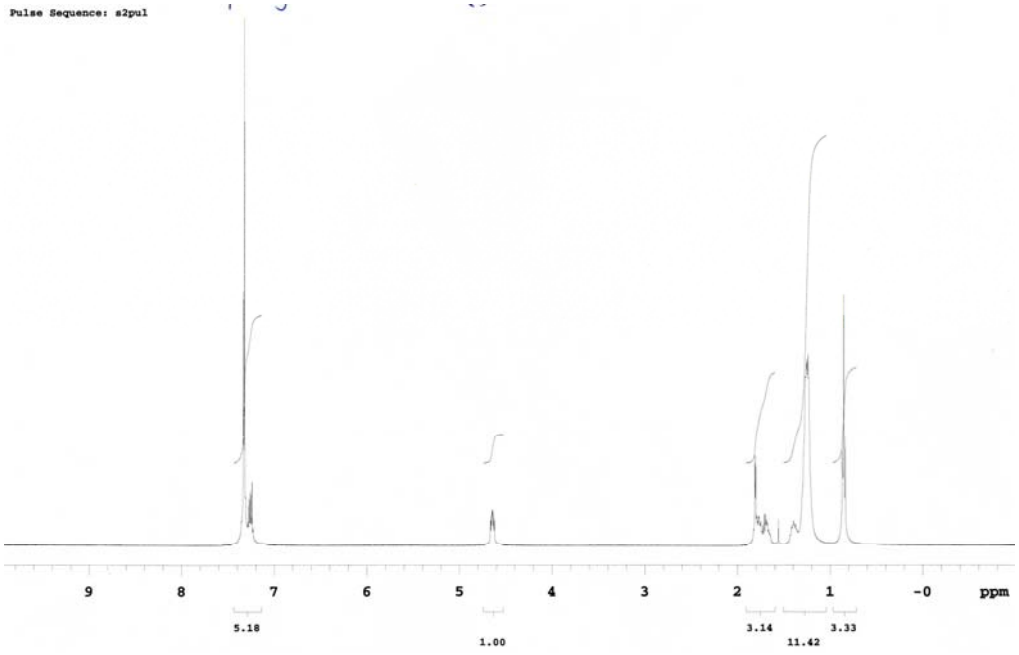

Figure S4 : ^{1}H NMR of 1-phenyl-1-octanol.

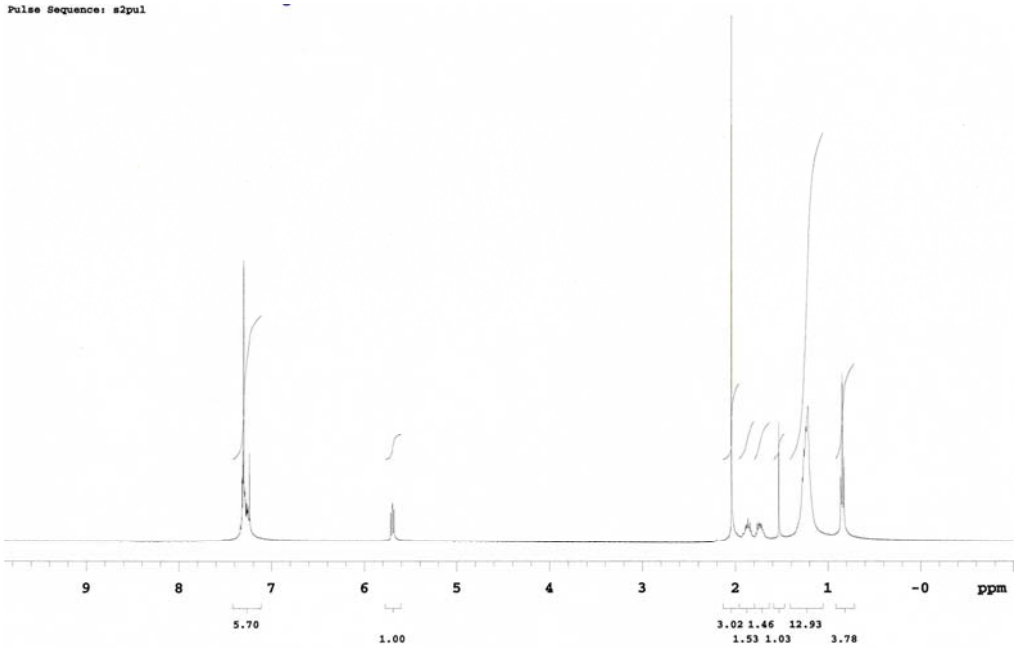

Figure S5 : ^{1}H NMR of 1-phenyl-1-octylacetate.

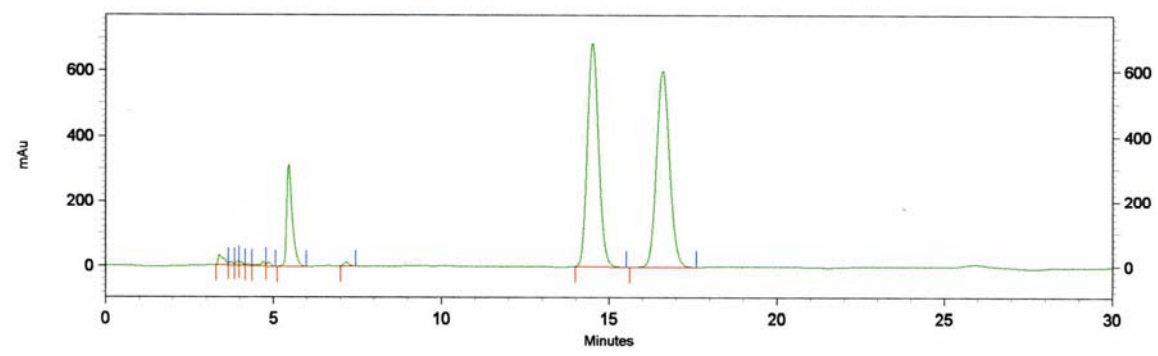

10	R-alcohol	14,492	16062387	43,334
11	S-alcohol	16,584	16328093	44,051

Figure S6 : HPLC trace of crude *rac*-1-phenyl-1-octanol.

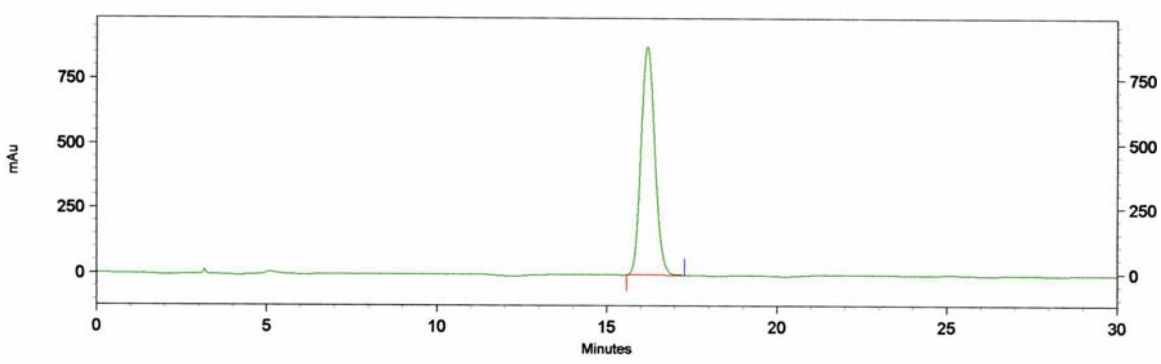

Figure S7 : HPLC trace of (*S*)-1-phenyl-1-octanol.

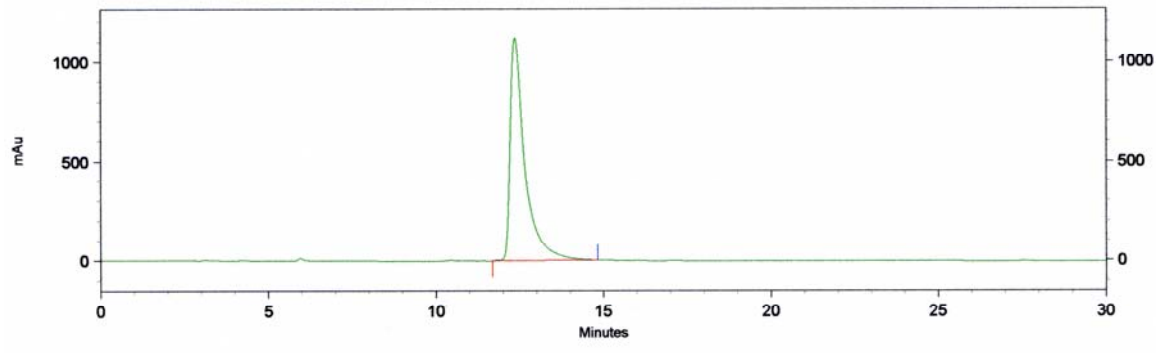

Figure S8 : HPLC trace of (*R*)-1-phenyl-1-octanol.

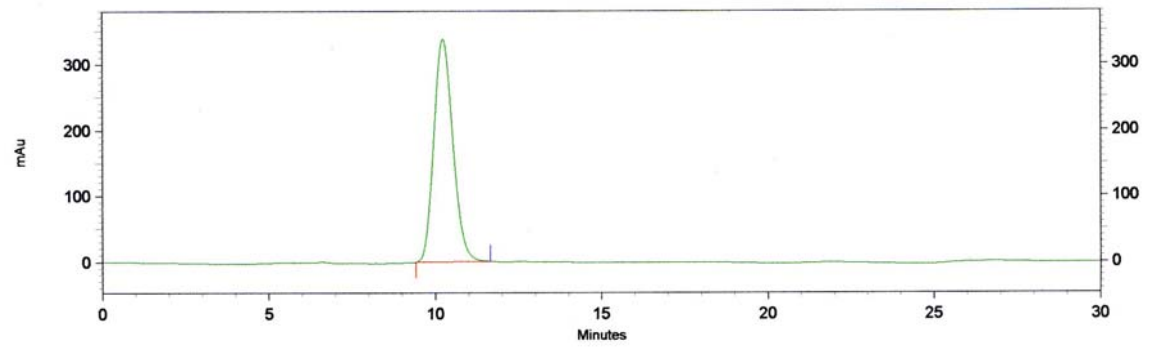

Figure S9 : HPLC trace of (*R*)-1-phenyl-1-octylacetate.

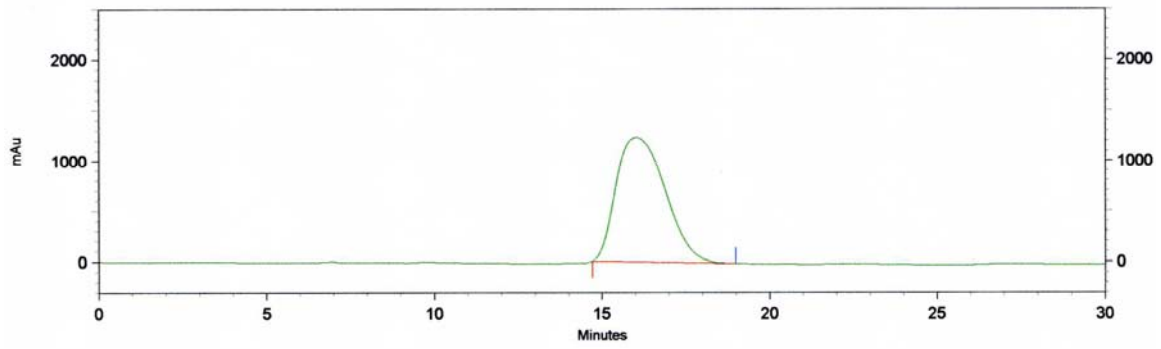

Figure S10 : HPLC trace of (*S*)-1-phenyl-1-octylacetate.

Enantiomerically pure (*S*)-1-phenyl-1-octanol and (*R*)-1-phenyl-1-octylacetate were obtained by deprotection of the (*S*)-acetate and acetylation of the (*R*)-alcohol, respectively.

UV/Vis and CD spectroscopy

Circular-dichroism (CD) spectra were recorded using a JASCO J-600 spectropolarimeter, where the sensitivity, time constant and scan-rate were chosen appropriately; UV/vis spectra were obtained using a Perkin Elmer Lambda 40P. A Peltier Temperature Programmer model 1 (PTP-1) was used to measure temperature variable UV/vis spectra between 0° and 80°. Measurements at low temperature were not possible at lower temperatures because the used solvents freeze at -5°C.

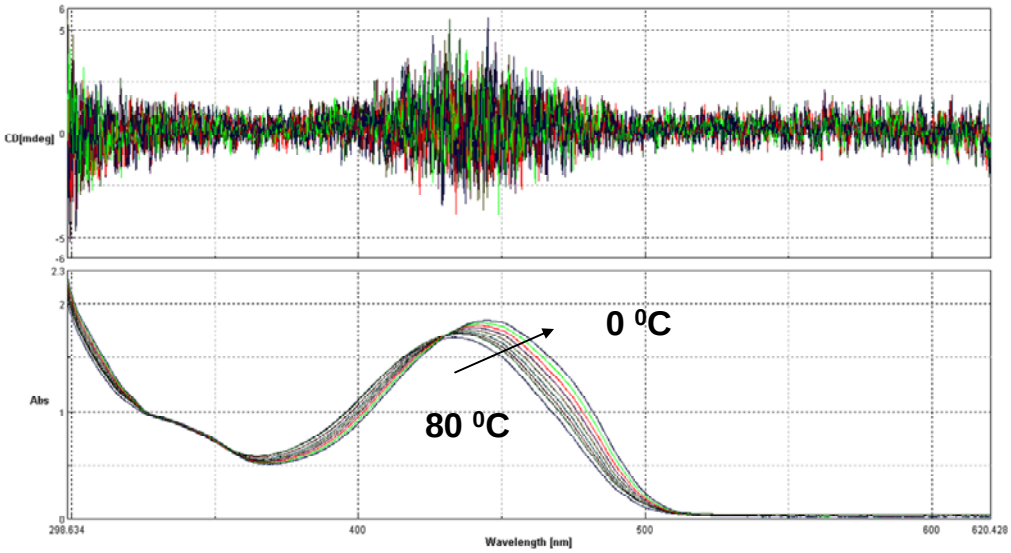

Figure S11 : CD spectra (top panel) and Uv/Vis spectra (bottom panel) of A-OPV4T in (*R*)-1-phenyl-1-octanol (2.7 x 10^{-4} M), for a range of temperatures comprised between 0° and 80°. The spectra have been registered in a 1 mm thick cuvette.

The concentration of the solution was chosen to be in the range of concentrations used for STM experiments. Over the range of temperatures checked, no CD effect was ever observed in any of the chiral solvents. CD spectra obtained in (*R*)-1-phenyl-1-octanol and (*R*)-1-phenyl-1-octylacetate are shown in figures S11 and S12, respectively (upper panel). Also at higher concentrations (with respect to the STM sample), there is no CD effect (not shown here).

The UV-vis spectra do not show any aggregation effect and only show conformational changes upon cooling.

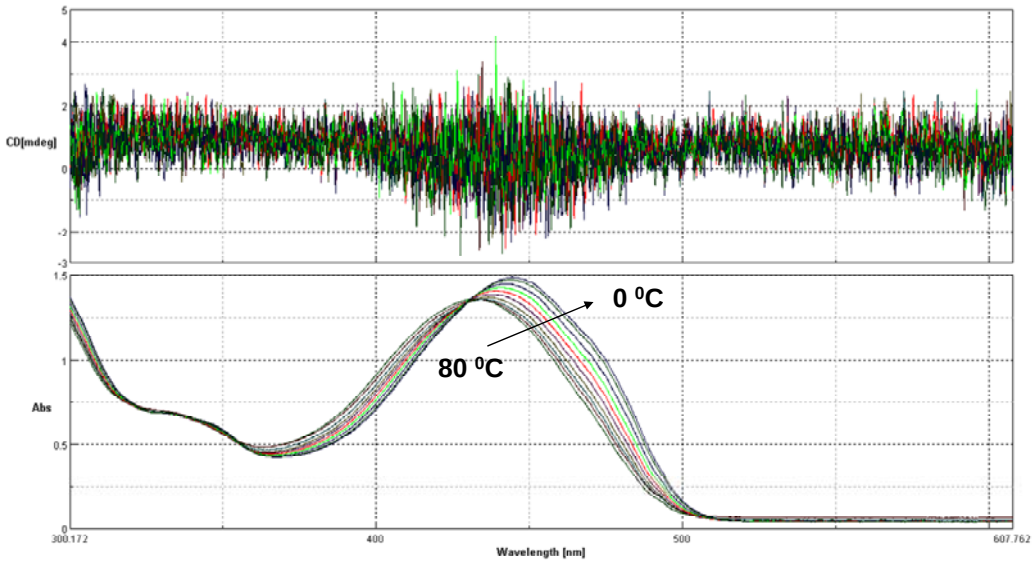

Figure S12 : CD spectra (top panel) and Uv/Vis spectra (bottom panel) of A-OPV4T in (*R*)-1-phenyl-1-octylacetate (2.0 x 10^{-4} M), for a range of temperatures comprised between 0° and 80°. The spectra have been registered in a 1 mm thick cuvette.

Scanning Tunneling Microscopy (STM)

Methods

STM imaging was performed at the solution - HOPG interface on two MI Picoscan (constant current mode) and on a Topometrix Discoverer (constant height mode). Images shown are subjected to a first-order plane-fitting procedure to compensate for sample tilt.

Complementary Images

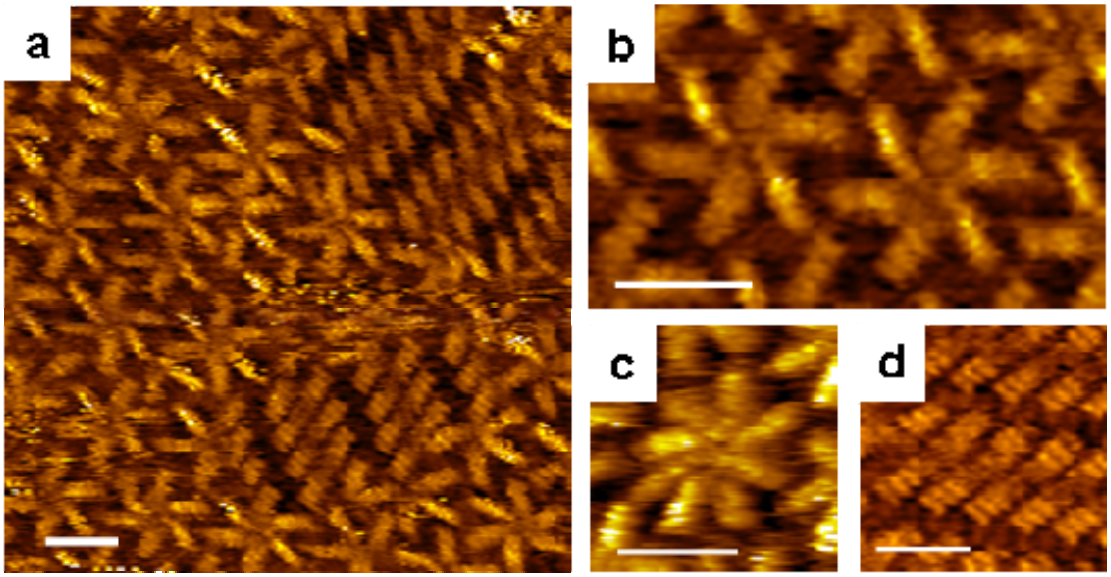

Figure S13 : STM images of A-OPV4T monolayer at the interface between a racemic mixture of (*R*)-1-phenyl-1-octanol and (*S*)-1-phenyl-1-octanol (rac-1-phenyl-1-octanol) and HOPG. Scale bars are 4 nm. a) On a large scale, rosettes are observed (left part of the image), as well as rows of dimers (right part of the image). b, c, d) Some typical surface aggregates obtained at the interface with rac-1-phenyl-1-octanol: rosettes, multimers, rows of dimers.

At the 1-phenyloctane - HOPG or *rac*-1-phenyl-1-octanol – HOPG interface, A-OPV4T mainly forms amorphous areas at the initial stages of the self-assembly process. The monolayers are characterized by large disordered areas, which in addition to dimers, tetramers and other (cyclic) oligomers also contains small ordered domains of rosettes. At longer times and dependent on the sample, larger areas of ordered rosettes were obtained. When using (*R*)-1-phenyl-1-octylacetate and (*S*)-1-phenyl-1-octylacetate as solvent, disordered monolayers with only locally small rosette domains were obtained.

STM images and emergence of structural order and homochirality as function of time at the (*R*)-1-phenyl-1-octanol - HOPG interface. This sequence of images has been recorded on the same sample as shown in Figure 3, though at a different location and starting about three hours later. In line with the expectations, the enantiomeric ratio is high from the beginning and does not evolve significantly in time.

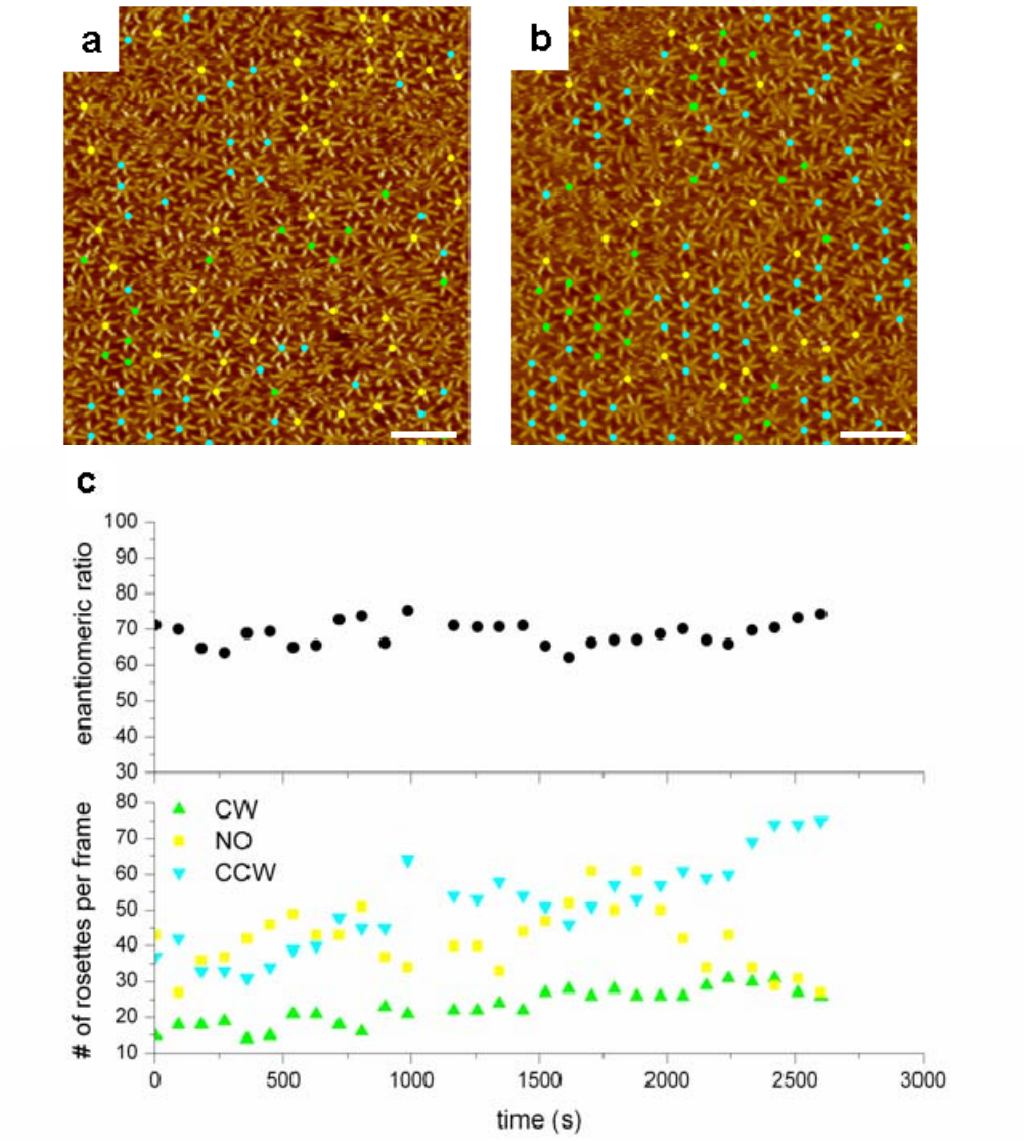

Figure S14 : a) First and b) last frame of a sequence of STM images of an A-OPV4T monolayer at the (*R*)-1-phenyl-1-octanol - HOPG interface recorded at the same area. The time gap between both frames is 43 minutes. Scale bar is 10 nm. The center of the rosettes is color-coded: CCW (blue), CW (green), NO (no-ordered) orientation (yellow) c) Evolution of the enantiomeric ratio (CCW/(CCW+CW)) and the number of rosettes of a given orientation (CCW, CW, or NO orientation) as a function of time. The corresponding movie is Supplementary Video2.

In this sequence of images of A-OPV4T recorded at the (*R*)-1-phenyl-1-octanol - HOPG interface, structural reorganisations are observed. For instance, the dimer pattern in A marked by the black square evolves into a rosette-like motif.

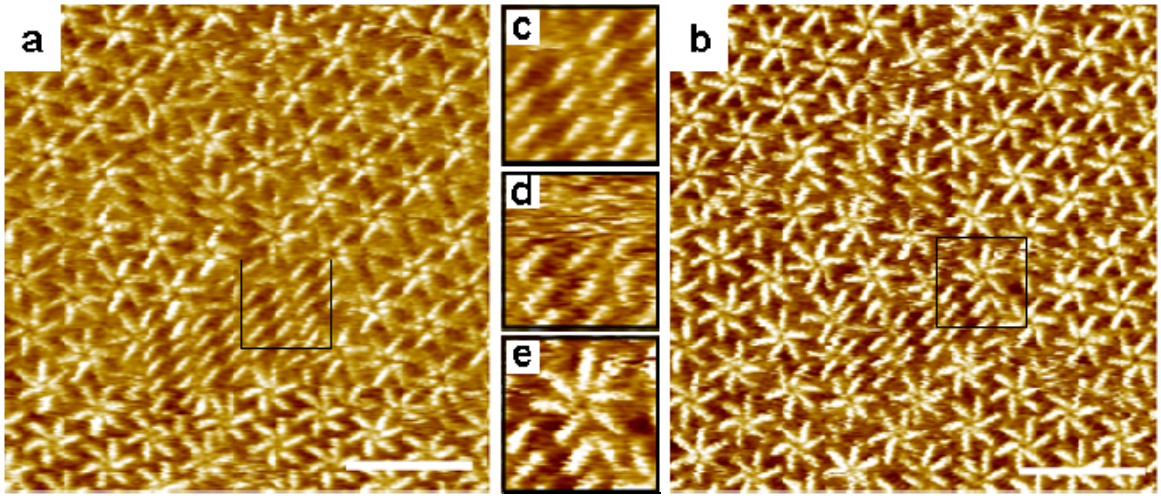

Figure S15 : a) First and b) last frame of a sequence of STM images of an A-OPV4T monolayer at the (*R*)-1-phenyl-1-octanol - HOPG interface recorded at the same area. The time gap between both frames is 117 seconds. Scale bar is 10 nm. The area of interest is indicated by the black square. A zoom of that area is shown in c) after 0 seconds, in d) after 48 seconds, and in e) after 117 seconds. In time, the dimer area indicated evolves into a rosette-like structure.

Complementary Movies

***Supplementary Video1*:** Sequence of images reflecting the emergence of structural order and chirality as a function of time. Snapshots of this movie and analysis are shown in Figure 3.

***Supplementary Video2*:** Sequence of images reflecting the emergence of structural order and chirality as a function of time. Snapshots of this movie and analysis are shown in Figure S14.